

# Supplementary Material

## 1 SUPPLEMENTARY DATA

The results of the molar flow rates for each radionuclide simulation (i.e., Cs, Cs with high inlet concentration, and U) are presented in Fig. S1, S2, and S3. Furthermore, mesh refinement results for each simulation are shown in Fig. S4, S5, and S6. Detailed plots about the fully coupled approach and the look-up table approach for each simulation are shown in Fig. S7, S8, and S9.

It is known that finite element solutions using the continuous Galerkin method have numerical instability problems, particularly in the cases of advection-dominated advection-diffusion problems and anisotropic diffusion problems. This can lead to non-physical oscillations at steep gradients and to local mass imbalance, as negative solute concentrations are cut off at zero for chemical calculations. In order to prevent spurious oscillations and negative concentrations, a variety of stabilization methods for finite element schemes have been developed (Burdakov et al., 2012; Mudunuru and Nakshatralla, 2017), such as the streamline-upwind Petrov–Galerkin (SUPG) stabilization method (Hughes, 1979; Brooks and Hughes, 1982), and the spurious oscillations at layers diminishing (SOLD) stabilization method (John and Knobloch, 2007; Kler et al., 2013), and flux-corrected transport scheme (Kuzmin and Turek, 2002; Kuzmin, 2009; Watanabe and Kolditz, 2015; Feng et al., 2019). In this work, we limit ourselves to isotropic diffusion problems. By using proper temporal and spatial discretization schemes, the approximate solution is kept stable, and few negative concentrations occur. We then follow the study of Hughes et al. (2000), estimating the local imbalance error in terms of the molar flow rate over internal nodes. As shown in Fig. S1–S3, the nodal molar flow rate is on the order of  $10^{-28}$  and below, which indicates local mass conservation is fulfilled.

In addition, the input data and results of the OpenGeoSys-6 models are conveniently provided via Jupyter-notebooks. They can be accessed in the OpenGeoSys-6 benchmarks collection in the official website: <https://www.opengeosys.org/>

## 2 SUPPLEMENTARY FIGURES

In Fig. S1, the molar flow rate of the Cs simulation with lower inlet concentration is shown. It is clear that the molar flow rate is extremely small, indicating acceptable mass conservation throughout the domain. In Fig. S2, a slightly molar flow rate of the Cs with higher inlet concentration simulation is shown. However, it is sufficiently small to neglect any influence on the simulation results. Furthermore, the molar flow rate of the U simulation, shown in Fig. S3 shows negligible influence on the mass conservation as well. The above is expected because a relative tolerance of  $1 \times 10^{-14}$  for the linear and non-linear solvers are set in each simulation.

Mesh refinement simulations were carried out to ensure reasonable concentration profiles. Fig. S4 shows the results of the Cs (lower inlet concentration) simulation. Both profiles agree quite well with the Euclidean norm  $\|c^{\text{coarse}} - c^{\text{fine}}\|_2 = (\sum_i |c_i^{\text{coarse}} - c_i^{\text{exact}}|^2)^{1/2}$  equal to  $1.65 \times 10^{-10}$ . In Fig. S5, the normal and refined mesh profiles for the Cs (high inlet concentration) are showed to have good agreement. The Euclidean norm is  $1.68 \times 10^{-7}$ . Finally, Fig. S6 shows the agreement of both coarser and finer simulations for U, with an Euclidean norm equal to  $1.89 \times 10^{-10}$ .

## 2.1 Figures

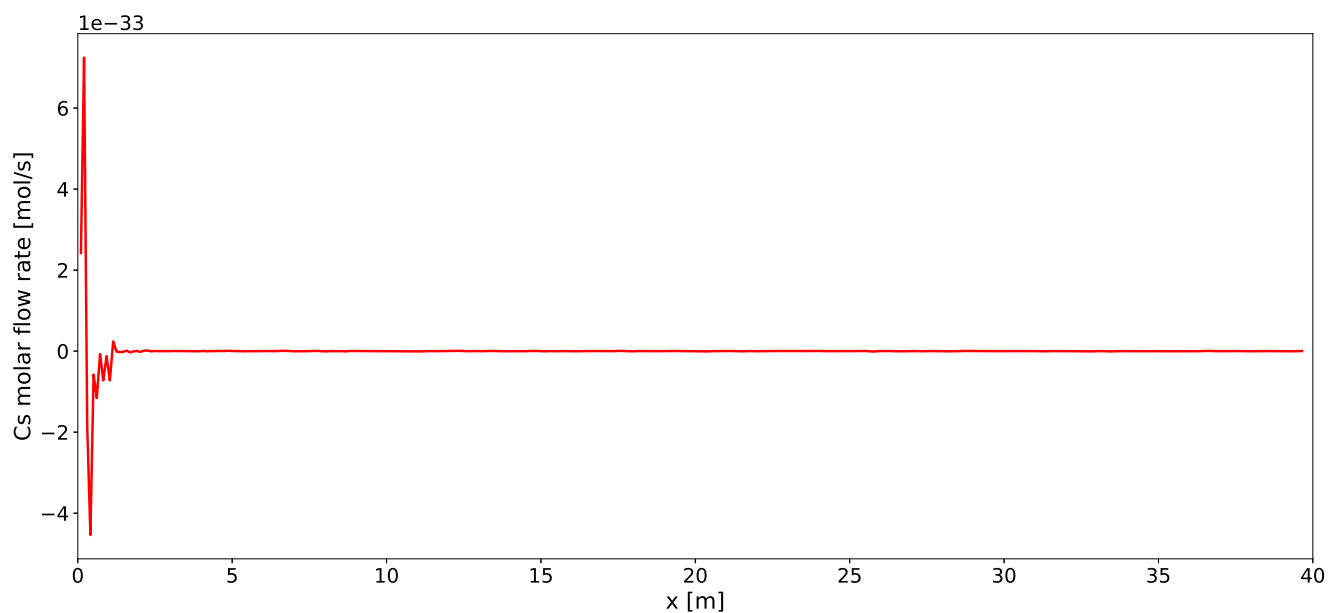


**Figure S1.** Molar flow rate of Cs at 1 million years. The plotted curve corresponds to the simulation with lower inlet concentration of  $1.019 \times 10^{-7}$  mol/kgw.

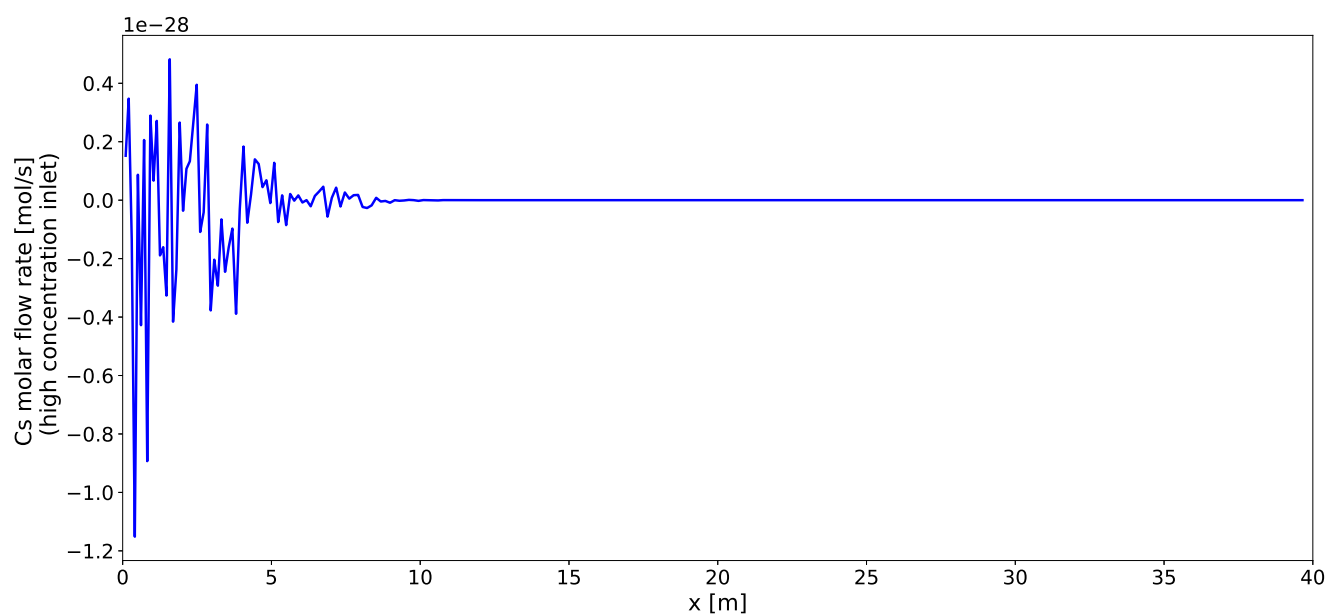


**Figure S2.** Molar flow rate of Cs at 1 million years. The plotted curve corresponds to the simulation with higher inlet concentration of  $1.019 \times 10^{-3}$  mol/kgw.

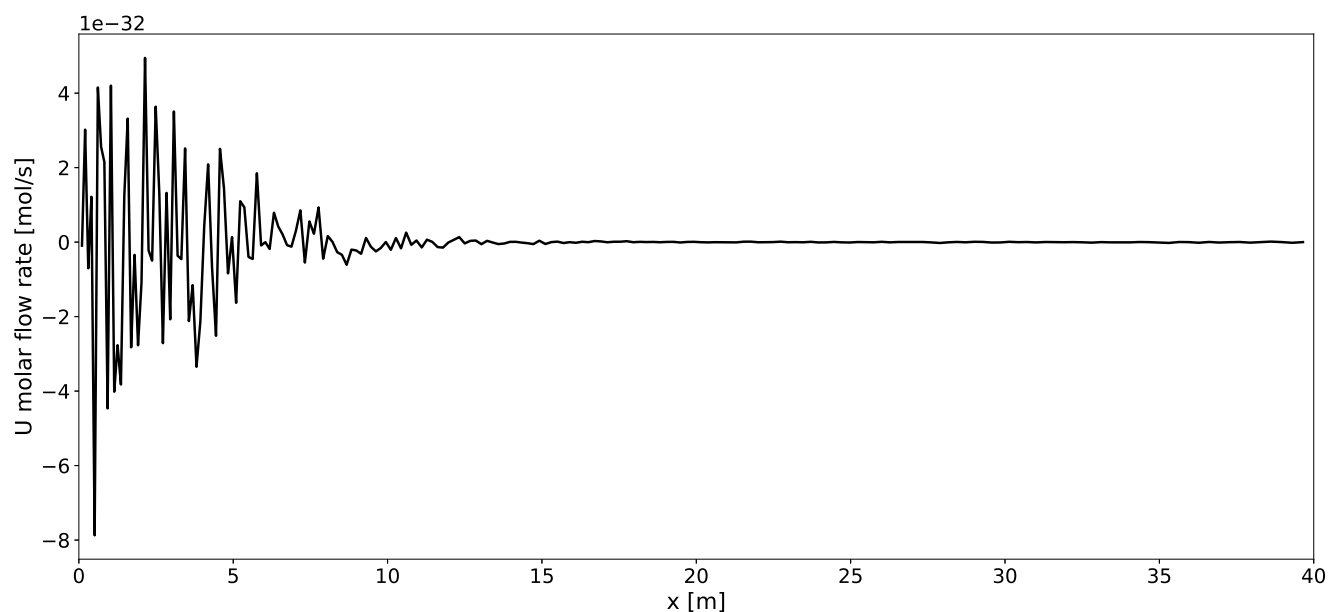


**Figure S3.** Molar flow rate of U at 1 million years.

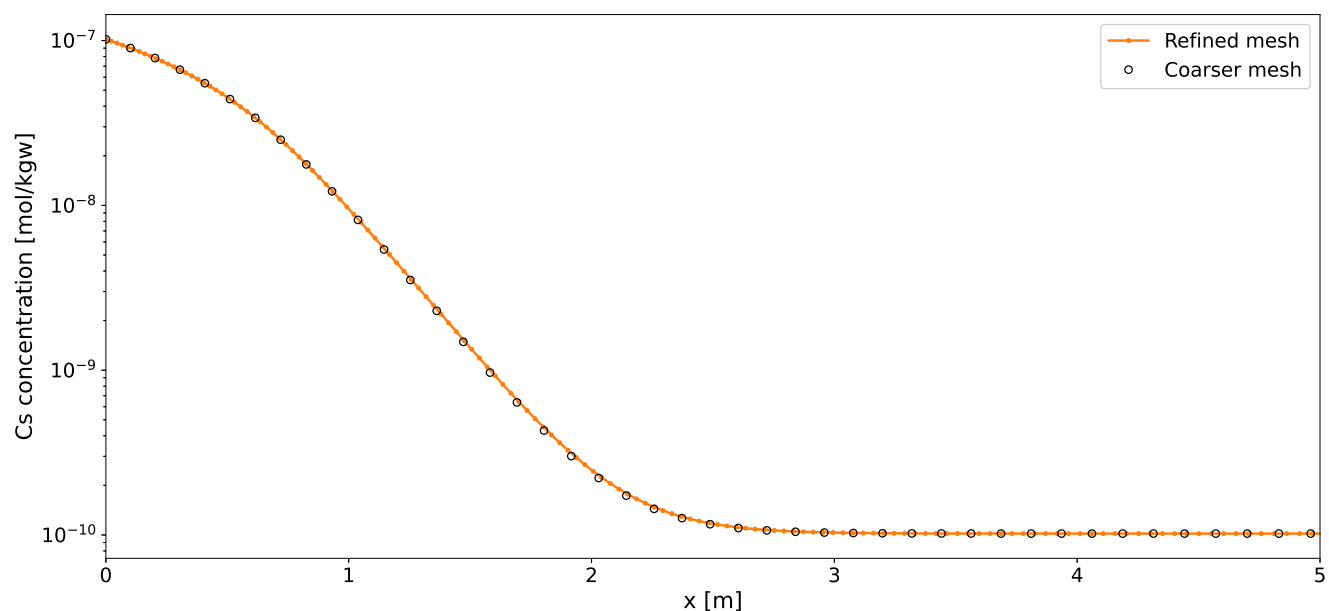


**Figure S4.** Comparison of the Cs concentration profiles with a coarser (default mesh used in the simulations) and a finer mesh. The coarser mesh has 200 elements, whereas the finer mesh is doubled (400 elements). The plotted curves corresponds to the simulation with lower inlet concentration of  $1.019 \times 10^{-7}$  mol/kgw.

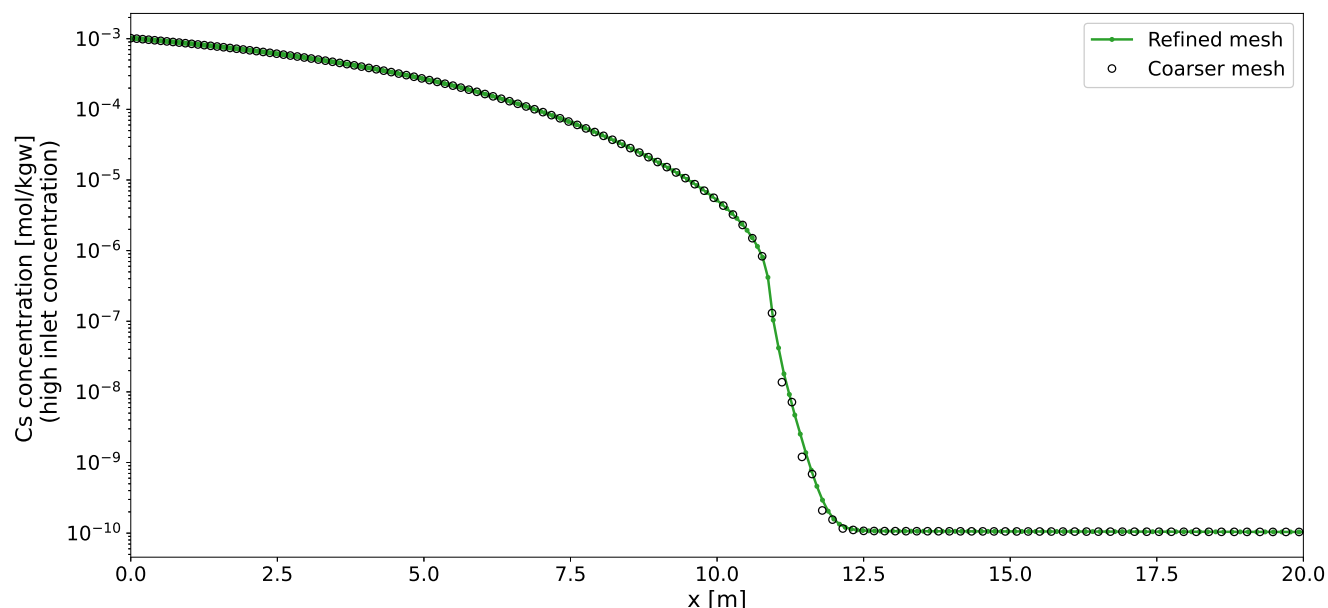


**Figure S5.** Comparison of the Cs concentration profiles with a coarser (default mesh used in the simulations) and a finer mesh. The coarser mesh has 200 elements, whereas the finer mesh is doubled (400 elements). The plotted curves corresponds to the simulation with higher inlet concentration of  $1.019 \times 10^{-3}$  mol/kgw.

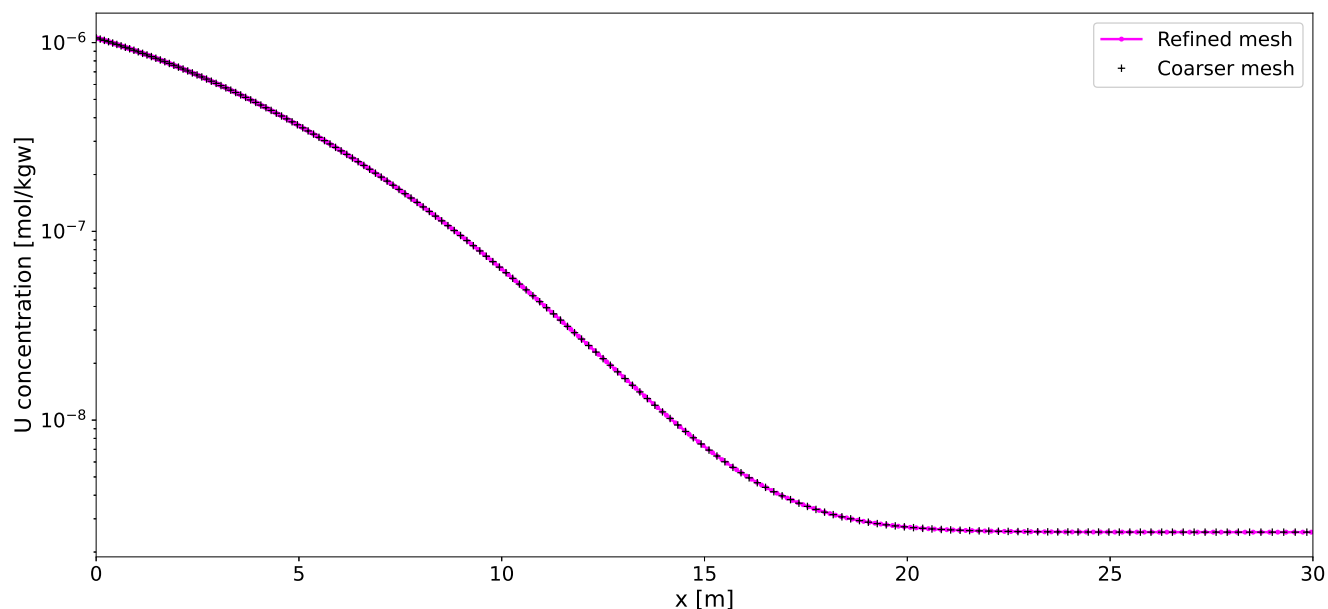


**Figure S6.** Comparison of the U concentration profiles with a coarser (default mesh used in the simulations) and a finer mesh. The coarser mesh has 200 elements, whereas the finer mesh is doubled (400 elements).

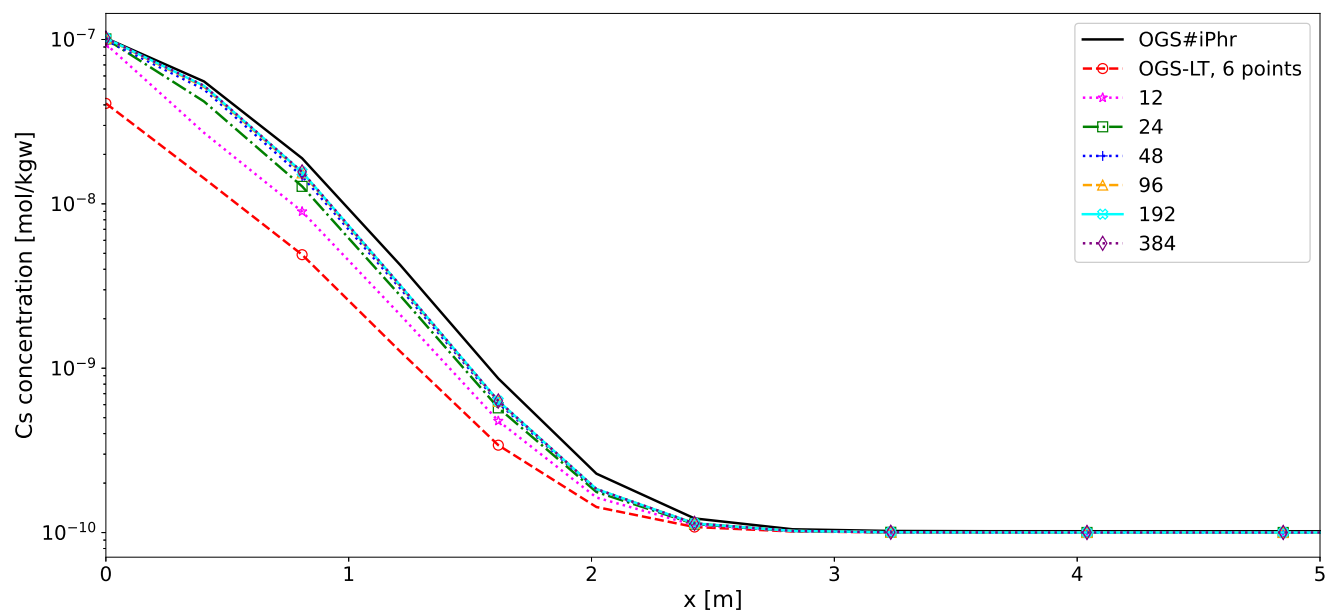


**Figure S7.** Comparison of the Cs concentration profiles using the fully coupled approach and the look-up table approach with different number of points.

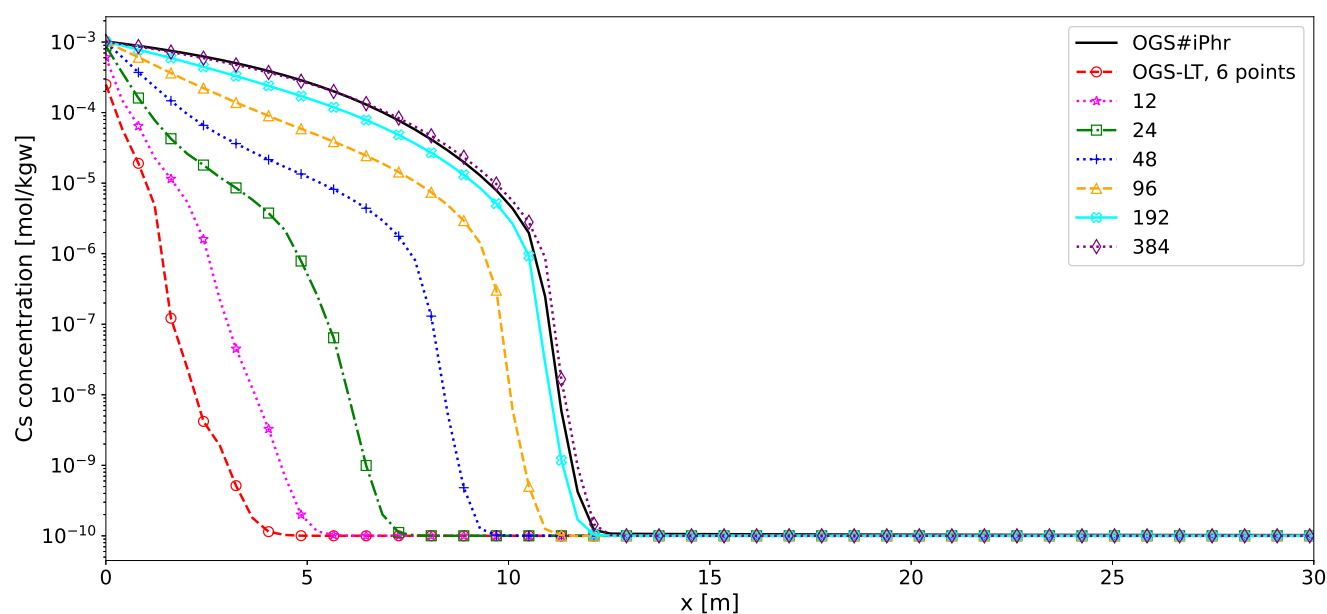


**Figure S8.** Comparison of the Cs concentration profiles (high inlet concentration) using the fully coupled approach and the look-up table approach with different number of points.

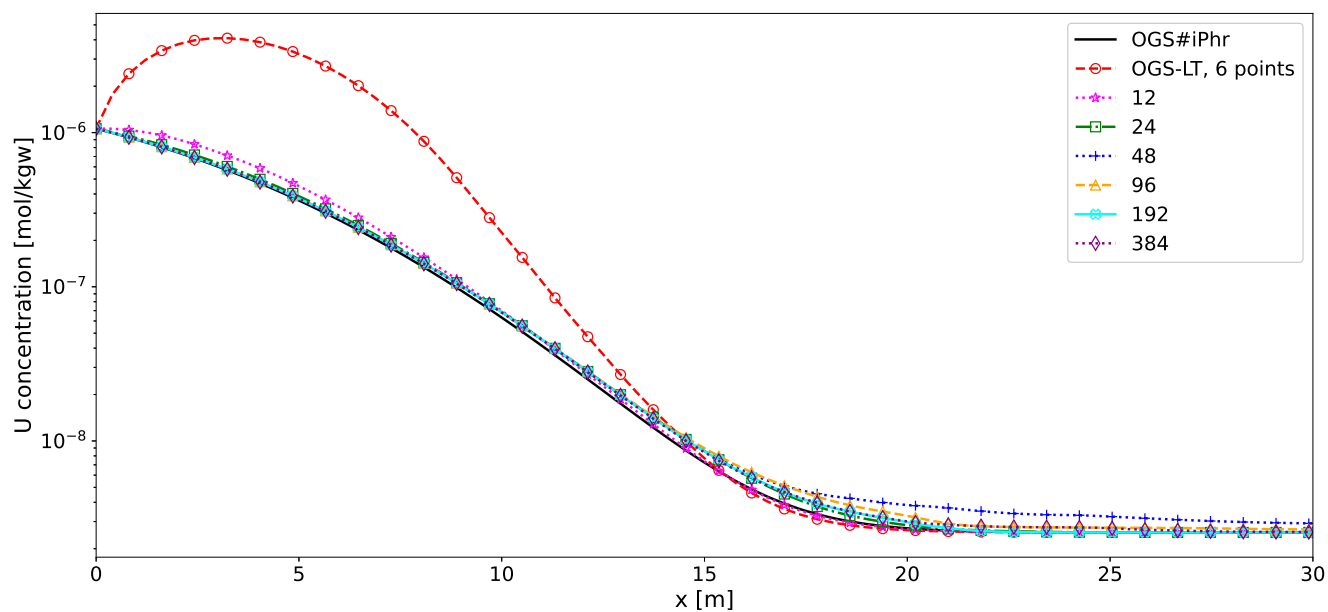


**Figure S9.** Comparison of the U concentration profiles using the fully coupled approach and the look-up table approach with different number of points.

## REFERENCES

- Burdakov O, Kapyrin I, Vassilevski Y. Monotonicity recovering and accuracy preserving optimization methods for postprocessing finite element solutions. *Journal of computational physics* **231** (2012) 3126–3142.
- Mudunuru M, Nakshatrala KB. On mesh restrictions to satisfy comparison principles, maximum principles, and the non-negative constraint: Recent developments and new results. *Mechanics of Advanced Materials and Structures* **24** (2017) 556–590.
- Hughes TJ. A multidimensional upwind scheme with no crosswind diffusion. *Finite element methods for convection dominated flows, AMD 34* (1979).
- Brooks AN, Hughes TJ. Streamline upwind/petrov-galerkin formulations for convection dominated flows with particular emphasis on the incompressible navier-stokes equations. *Computer methods in applied mechanics and engineering* **32** (1982) 199–259.
- John V, Knobloch P. On spurious oscillations at layers diminishing (sold) methods for convection–diffusion equations: Part i—a review. *Computer methods in applied mechanics and engineering* **196** (2007) 2197–2215.
- Kler PA, Dalcin LD, Paz RR, Tezduyar TE. Supg and discontinuity-capturing methods for coupled fluid mechanics and electrochemical transport problems. *Computational Mechanics* **51** (2013) 171–185.
- Kuzmin D, Turek S. Flux correction tools for finite elements. *Journal of Computational Physics* **175** (2002) 525–558.
- Kuzmin D. Explicit and implicit fem-fct algorithms with flux linearization. *Journal of Computational Physics* **228** (2009) 2517–2534.
- Watanabe N, Kolditz O. Numerical stability analysis of two-dimensional solute transport along a discrete fracture in a porous rock matrix. *Water Resources Research* **51** (2015) 5855–5868.
- Feng D, Neuweiler I, Nackenhorst U, Wick T. A time-space flux-corrected transport finite element formulation for solving multi-dimensional advection-diffusion-reaction equations. *Journal of Computational Physics* **396** (2019) 31–53.
- Hughes TJ, Engel G, Mazzei L, Larson MG. The continuous galerkin method is locally conservative. *Journal of Computational Physics* **163** (2000) 467–488.